

# NON-PARAMETRIC STATISTICS AS A TOOL FOR PROVENANCE ANALYSIS IN GRAVEL DEPOSITS: VINCHINA FORMATION (MIOCENE, ARGENTINE) AS A STUDY CASE

Marianela Díaz<sup>1,2</sup>, Sergio A. Marensi<sup>3</sup>, Carlos O. Limarino<sup>3</sup>

<sup>1</sup> Centro de Investigaciones de la Geósfera y Biosfera CIGEOBIO (CONICET/UNS), San Juan, Argentina. marianelaxy.diaz@gmail.com

<sup>2</sup> Departamento de Geología, Facultad de Ciencias Exactas, Físicas y Naturales (UNS), San Juan, Argentina.

<sup>3</sup> Instituto de Geociencias Básicas, Aplicadas y Ambientales de Buenos Aires (UBA-CONICET), Ciudad Autónoma de Buenos Aires, Argentina.

## ARTICLE INFO

### Article history

Received July 15, 2020

Accepted October 5, 2020

Available online October 13, 2020

### Handling Editor

Fernando Gómez

### Keywords

Statistical analysis

Provenance

Conglomerates

Vinchina Formation

Miocene

## ABSTRACT

The Neogene Vinchina Basin developed between 27 and 33°S as a foreland basin as a response to the Andean deformation in the southern part of the Central Andes. The Miocene Vinchina Formation (Turner, 1964) was deposited mainly in fluvial, fluvial-eolian, eolian, and lacustrine environments, reaching up to 6400 m in thickness representing the main depositional unit in the basin. This unit is remarkably exposed along the Sierra de Los Colorados (La Rioja Province, Argentina), where this study was carried out.

The results from statistical analyses from 33 gravel beds, their modal compositions, compositional trends, and distribution patterns, based on in-situ lithological clast-counting, are presented. The statistical approach was carried out by using hierarchical clustering and principal components analysis (PCA), which permitted differentiating three compositional clusters thought to represent different petrofacies. The first cluster involves samples with compositions widely dominated by neovolcanic andesitic clasts, where intrabasinal volcanic effusions were the main detrital source. The second one comprises samples with mixed compositions dominated by paleovolcanic clasts. Detrital sources of this cluster were primarily the cordilleran/precordilleran area, with subordinated contributions from the Western Sierras Pampeanas crystalline basement and intrabasinal volcanic deposits. The third cluster involves mixed samples with a dominance of crystalline-basement supply. The main source area for these samples was the Western Sierras Pampeanas, although the cordilleran/precordilleran supply is present in significant proportions.

This study illustrates the merit of using non-parametric statistics in provenance studies, especially to detect internal compositional variations when multiple source areas are active.

## INTRODUCTION

Basin sedimentary record is a beneficial tool when reconstructing the climatic and tectonic evolution of foreland basins and their source areas.

In particular, the study of basin-fill deposits has proven to be efficient in better knowing the evolution of the Andean orogen and its related basins, where the tectonic imprint often makes difficult the interpretation of their geologic history.

The classic approach in assessing of conglomeratic deposits relies on their sedimentological, lithological, and/or paleontological characteristics, which aim to compare age or paleoenvironmental conditions. Provenance studies have traditionally been based on modal clast composition and its internal variations (Howard, 1993). Thus, provenance interpretations rely mainly on the accurate recognition of the different clast lithologies and a good understanding of the main possible source areas and source rocks. This widely used approach faces serious troubles where different source areas share similar lithologies. Andean foreland basins are commonly fed by detritus from the fold-and-thrust belt (DeCelles and Giles, 1996; among others) and the Andean volcanic arc (Jordan *et al.*, 2001; Varela *et al.*, 2013). Most recently, Capaldi *et al.* (2017) indicated that in distal broken segments of the foreland basin, the regional provenance signatures from fold-and-thrust belt and hinterland areas are diluted by local contributions from basement-cored uplifts. In the study area, the fold-and-thrust belt corresponds to the Precordillera geological province, and the Andean volcanic arc constitutes the geological provinces of Cordillera Frontal and Principal. Basement-cored uplifted blocks in the area depict Sierras Pampeanas Noroccidentales. On the other hand, non-parametric statistical methods have proven good results in discriminating source areas and compositional trends (Ciampalini *et al.*, 2011; Limarino and Giordano, 2016).

This study presents a new approach in understanding compositional changes and trends in a broken-foreland basin, where detrital source areas that shared some lithologies remained nearly static during the basin evolution. The Vinchina Formation was deposited during the Miocene in the Vinchina broken-foreland basin, which developed in the Western Sierras Pampeanas province (Figure 1) in La Rioja Province, northwestern Argentina. The basin developed as a response of combined thin-skinned and thick-skinned deformation (Beer and Jordan, 1989; Jordan *et al.*, 1993; Milana *et al.*, 2003; Japas *et al.*, 2015, 2016). In this regard, the classic evolutionary model of foreland basins (Jordan *et al.*, 2001) includes a “simple foreland basin” that changes into a “broken-foreland basin” due to its subdivision into smaller sub-basins. In this model, the simple foreland stage results from the flexural response to the Miocene Andean tectonic shortening.

The broken-foreland stage developed during the tectonic uplift of basement blocks of Western Sierras Pampeanas through high-angle reverse faults, which fragmented the previous continuous basin into smaller ones, being the Vinchina Basin one of them (Jordan and Allmendinger, 1986).

The methodology here presented demonstrates the effectiveness of non-parametric statistics in quantifying variations in clast compositions and the similarities and dissimilarities between compositional groups, which in turn, are interpreted in terms of provenance and basin evolution. Similar works have been presented by Ciampalini *et al.* (2011), Limarino and Giordano (2016), and Vermeesch *et al.* (2016), obtaining satisfactory results in differentiating multiple source areas in modern and ancient, extensional and compressional settings.

## GEOLOGICAL SETTING

This Vinchina Basin is bounded to the west by the Cordillera Frontal and the Precordillera through the Bolsón de Jagüé valley, to the east by the Valle Hermoso valley and the Nevados del Famatina Range, and the north and south by basement blocks belonging to the Western Sierras Pampeanas (Sierra de Toro Negro and Umango-Espinal arch respectively; Fig. 1A). This depocenter locates in a structurally complex area, where two megashear zones converge: the Desaguadero-Valle Fértil (DVFL) and Tucumán (TL) lineaments. The former has an NNW strike and a sinistral movement component, whereas the latter has an NE strike and dextral component (Fig. 1A). These lineaments respond to old suture zones (Toselli *et al.*, 1985), which form an intricate deformation pattern. Minor structures affecting the study area are Las Minitas Lineament (LML) and Famatina Fracturing System (FFS), as reported by Japas *et al.* (2015, 2016).

The geologic setting of the study area comprises volcanic, sedimentary, and metamorphic rocks, which outcrop in four morphotectonic units, namely Cordillera Frontal, Precordillera, Western Sierras Pampeanas, and Famatina range (Figs. 1B and 2). Although Limarino *et al.* (2010) proposed the existence of a Protofamatina range during the late Miocene, previous works (Tripaldi *et al.*, 2001; Schencman *et al.*, 2018) discarded the Famatina range as a source area for the Vinchina Formation on the basis of paleocurrent data and paleogeographic

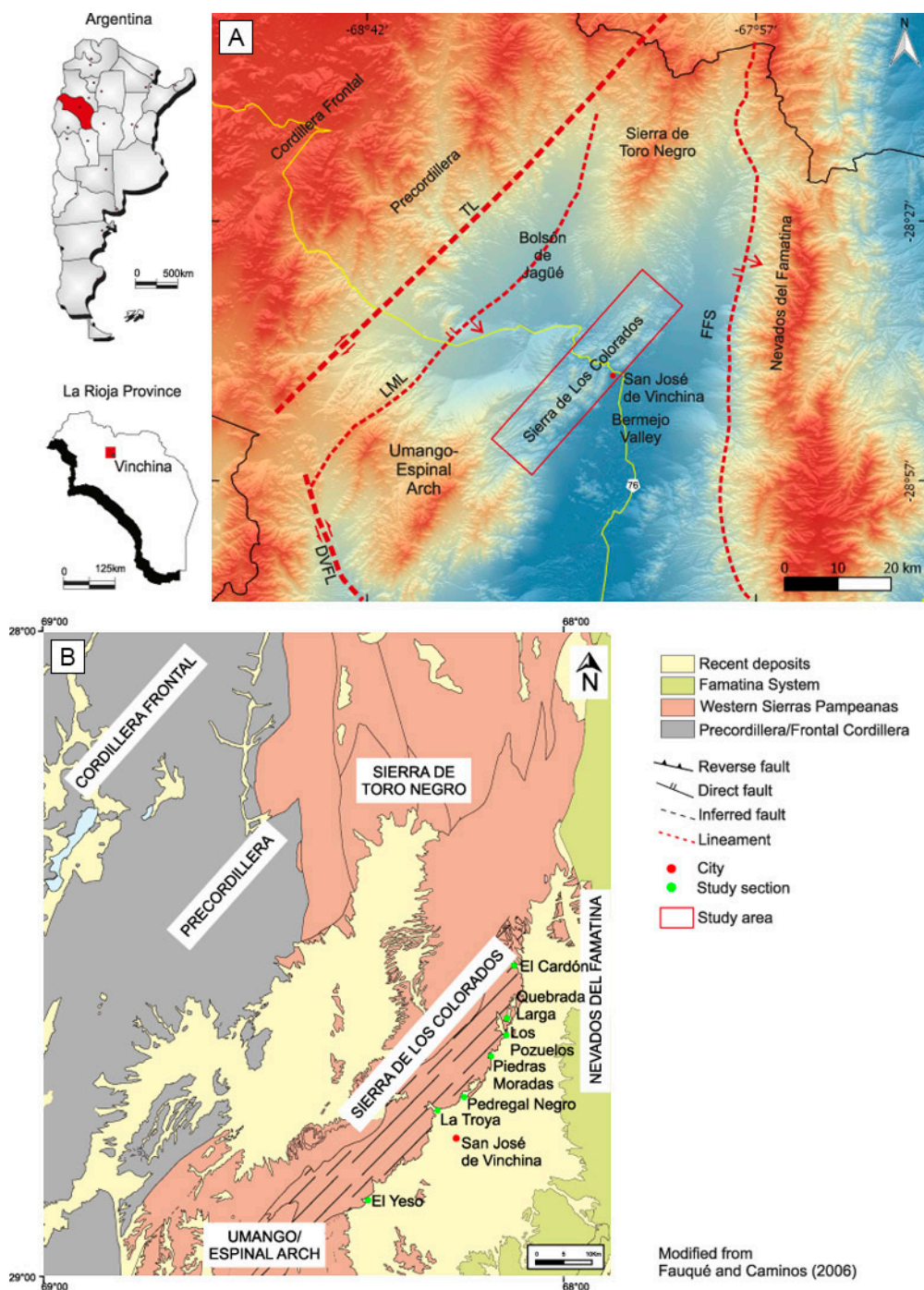


**Figure 1.** Location map of the study area. **a)** Digital Elevation Model showing the main structural lineaments (modified from USGS database); TL: Tucumán Lineament; DVFL: Desaguadero-Valle Fértil Lineament; LML: Las Minitas Lineament; FFS: Famatina Fracturing System. **b)** Simplified geologic map depicting major morphotectonic units in the area (modified from Fauqué and Caminos, 2006). Striped zone highlights Vinchina Formation outcrops. The green circle indicates study sections, named (from north to south) “El Cardón”, “Quebrada Larga”, “Los Pozuelos”, “Piedras Moradas”, “Pedregal Negro”, “La Troya”, and “El Yeso”. The red circle indicates the closest city to the study area (San José de Vinchina).

**Figura 1.** Mapa de ubicación del área de estudio. **a)** Modelo de elevación digital y principales lineamientos estructurales (modificado de USGS); TL: Lineamiento Tucumán; DVFL: Lineamiento Desaguadero-Valle Fértil; LML: Lineamiento Las Minitas; FFS: Sistema de Fracturación de Famatina. **b)** Mapa geológico simplificado mostrando las principales unidades morfoestructónicas en el área (modificado de Fauqué and Caminos, 2006). La zona rayada indica los afloramientos de la Formación Vinchina. El círculo verde indica las localidades de estudio relevadas, denominadas (de norte a sur) “El Cardón”, “Quebrada Larga”, “Los Pozuelos”, “Piedras Moradas”, “Pedregal Negro”, “La Troya” y “El Yeso”. El círculo rojo indica la ciudad más próxima al área de estudio (San José de Vinchina).

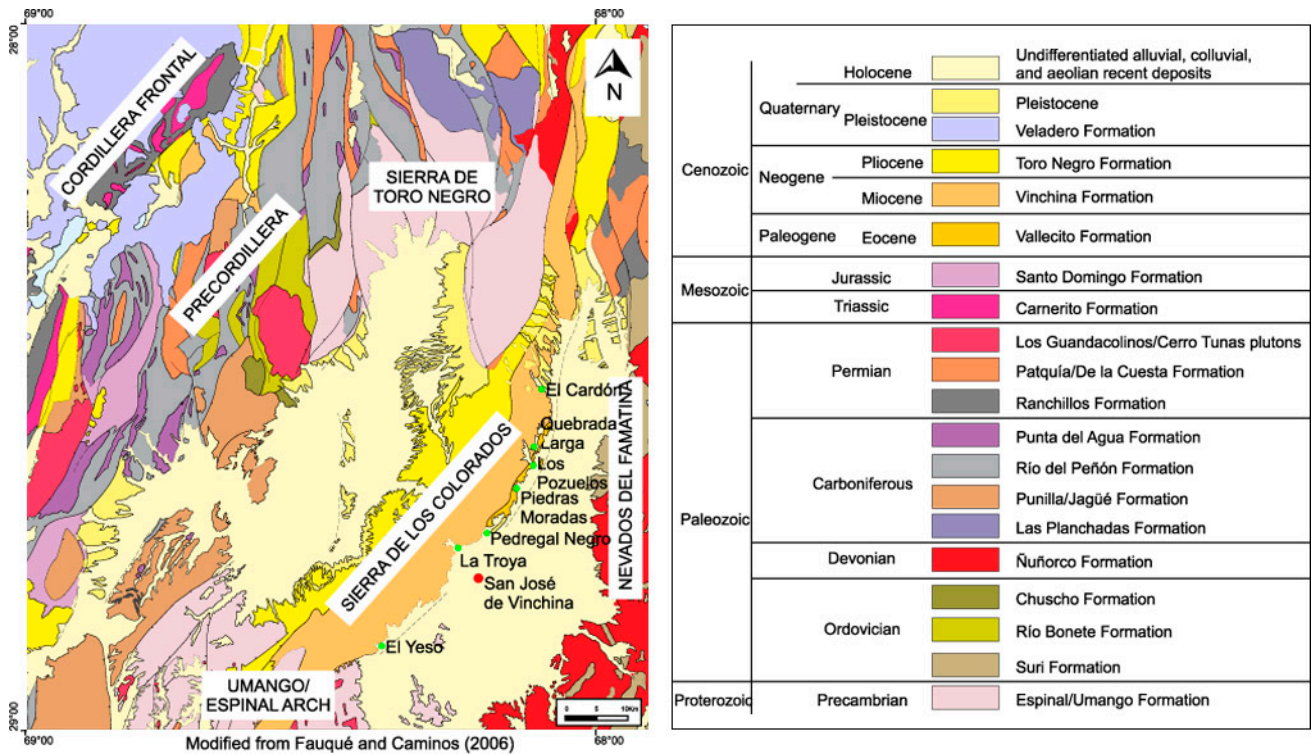


**Figure 2.** Geologic map of the study area depicting the dominant lithologies at each morphotectonic unit (modified from Fauqué and Caminos, 2006).

**Figura 2.** Mapa Geológico del área de estudio mostrando las litologías dominantes en cada una de las unidades morfoestructónicas (Modificado de Fauqué y Caminos, 2006).

reconstructions from sedimentary facies analysis. A brief description of each morphotectonic unit's stratigraphy is presented next, although the reader should refer to Fauqué and Caminos (2006) for a detailed characterization of each unit.

The Cordillera morphotectonic unit exhibits primarily igneous volcanic and volcanic-derived rocks, and minor granitic rocks. Pre-Miocene units are the Ranchillos (upper Carboniferous-Permian) and Carnerito (Permian-Triassic) formations. The former comprises volcanic breccias, conglomerates, and agglomerates, with minor greenish sandstones and mudstones. The latter is made up of granites, rhyolites, and rhyodacites.

The Western Sierras Pampeanas corresponds to tectonically uplifted basement-cored blocks located to the north (Sierra de Toro Negro) and south (Umango-Espinal arch) of the basin. The Espinal Formation (Precambrian-Mesoproterozoic) outcrops in both blocks and constitutes the primary crystalline unit in the area. It comprises medium to high-grade metamorphic rocks, which vary from green schists facies to amphibolite and granulite

facies. Granites, granodiorites, and tonalites form a late intrusive phase. The Umango Formation (Precambrian-Neoproterozoic) is also composed of metamorphic rocks, which are represented by gneisses, amphibolites, granulites, mafic dykes, and metagabres. The Paleozoic to Cenozoic record comprises volcanic, granitic plutons and sedimentary rocks. The Las Planchadas Formation (early Carboniferous) comprises volcanic and volcanoclastic acidic to intermediate rocks such as tuffs, ignimbrites, and volcanic breccia deposits, along with andesitic, dacitic, and rhyolitic flows and basaltic pillow lavas. Organic-rich mudstones accompany these rocks. The granitic plutons intruded the crystalline basement during the Carboniferous, and they correspond mainly to pink-grey to reddish granitic, granodioritic, tonalitic, and dioritic bodies, which are known as Cerro Las Tunas, Potrerillos, and Los Guandacolinos plutons. The Río del Peñón and Patquía/De la Cuesta formations (Upper Carboniferous-Lower Permian) occur here, and they comprise the remnant outcrops of Paganzo Basin in Western Sierras Pampeanas. The Río del Peñón

Formation comprises grey and pink conglomerates and sandstones with minor greenish mudstones. The overlying Patquía/De la Cuesta Formation comprises arkosic medium to coarse-grained sandstones, mudstones, scarce conglomerates, and evaporitic layers. The Vallecito Formation (Eocene) crops out at the northern and central sectors of Sierra de Los Colorados. This unit comprises a well-sorted medium to fine-grained reddish sandstones deposited in eolian environments interpreted as dunes and draas. This unit is separated from the overlying Vinchina Formation by an erosive unconformity.

The La Rioja Precordillera exhibits several sedimentary (and metasedimentary) and igneous rocks. The oldest units are Río Bonete (sedimentary) and Chuscho (volcanic) formations, both of Ordovician age. Río Bonete Formation comprises massive fine-grained and laminated limestones, dark quartzites, micaceous schists, chloritic schists, and black and green mudstones. This unit intercalates with basaltic pillow lavas of the Chuscho Formation, and the group was interpreted by Fauqué and Villar (2003) as the Ophiolitic Belt of Western Precordillera. The Punilla/Jagüé Formation (Upper Devonian-early Upper Carboniferous) appears as an elongated NNE-SSW belt in the eastern flank of the Precordillera, and it is made up of greenish-grey conglomerates, wackestones, mudstones, and diamictites. Overlying the Jagüé Formation, the lower-Carboniferous Punta del Agua Formation is composed of volcanic (andesites and rhyodacites) and volcanoclastic rocks (pyroclastic flows, volcanic conglomerates, and volcanic lithic sandstones). The Río del Peñón and Patquía/De la Cuesta Formation (Upper Carboniferous-Lower Permian), which were previously characterized, are also registered in the Precordillera. The Santo Domingo Formation (Upper Triassic-Lower Jurassic) occurs in the western flank of the Precordillera. It is composed of conglomerates, sandstones, and gypsum layers, which are interlayered with basaltic flows. During the Cenozoic, the Precordillera and Western Sierras Pampeanas were sites of continental deposition. In the Precordillera, the Vallecito Formation (Eocene) is well represented, particularly in San Juan (e.g., Huaco area) and southernmost La Rioja (e.g., Cordon de La Flecha area) provinces (southwards of the study area), where it involves red and reddish medium- to fine-grained eolian sandstones.

Previous works indicate that the Vinchina

Formation was deposited in a broken-foreland basin during the Andean orogeny (Limarino *et al.*, 2001; Ciccioli *et al.*, 2011). Sedimentation took place mainly in fluvial, alluvial, eolian, and lacustrine environments (Tripaldi *et al.*, 2001; Limarino *et al.*, 2001, Schencman *et al.*, 2018). The thickness of the Vinchina Formation varies along the depositional strike, from 4273 m at the Quebrada Larga section to 6451 m at the El Yeso section. In this matter, the mean thickness of the lower member is 1600 m, whereas the mean thickness of the upper member is 2950 meters.

The Vinchina Formation was divided initially into two informal members, namely, lower and upper, on the basis of their lithological characteristics Ramos (1970; Fig.3). Later, Marensi *et al.* (2015) identified seven third-order depositional sequences bounded by unconformities. More recently, Schencman *et al.* (2018) divided the paleoenvironmental evolution of the Vinchina Formation into four stages. Stage 1 involves the basal beds, and it is characterized by the development of ephemeral braided fluvial systems (with eolian reworking) and sandflats, under arid climatic conditions. Stage 2 comprises the rest of the lower member, which is dominated by fluvial transport with multichannelized (anastomosed) and non-confined (terminal lobes) systems ending in playa lakes, under less arid conditions than the previous stage. An important deformational event, followed by a deep incision, is represented by the unconformity that separates the two members (Marensi *et al.*, 2000). Evolutionary stage 3 comprises the lower third of the upper member, and gravely-sand braided fluvial systems characterize it in the northern part of the basin, which changes to sandy-gravel braided systems and meandering systems in the central part, and grade to anastomosed systems and fluvial-eolian interaction systems towards the southern sector. During this time, the southern area was distinguished by a sandy-muddy plain dominated by unconfined rivers, whereas in the northern and central sectors, rivers were moderately confined. Stage 4 involves the rest of the upper member, and it is characterized by the development of meandering fluvial systems in the central sector of the basin, which provided a significant amount of fine-grained sediments to ephemeral clastic-evaporitic lakes which developed under arid conditions in the southern part of the basin (Ciccioli, 2008). In order to simplify stratigraphic references

along the text, it is necessary to highlight that: (1) the lower part of the lower member is equivalent to the depositional sequence 1 of Marensi *et al.* (2015); (2) the upper part of the lower member refers to sequence 2 of the above-mentioned work; (3) the lower part of the upper member corresponds to depositional sequences 3 and 4 of the cited work; and (4) the upper part of the upper member comprises sequences 5, 6, and 7 of Marensi *et al.* (2015).

The Miocene age of Vinchina Formation has been recently improved based on U/Pb dating of volcanic and detrital zircons. Ciccioli *et al.* (2014) reported a sedimentation age of  $15.6 \pm 0.4$  My, obtained from detrital zircons collected from a tuffaceous sandstone located a few meters above the base of the unit. More recently, Stevens Goddard and Carrapa (2017) and Collo *et al.* (2017) registered maximum sedimentation ages of  $18.6 \pm 0.4$  My and  $12.62 \pm 0.4$  My from detrital zircons obtained from samples at the lower and middle part of the lower member. On the other hand, Ciccioli *et al.* (2014) reported a depositional age of  $9.24 \pm 0.034$  My for the upper part of the upper member, on the basis of data obtained from volcanic zircons in a tuffaceous level. Additionally, Amidon *et al.* (2016) indicated that the depositional age of Vinchina Formation has to be older than 6.9 My, based on U/Pb ages from the lowermost levels of the overlying Toro Negro Formation.

## METHODOLOGY AND DATA

The evolution of broken-foreland basins and their source areas can be interpreted by assessing the sedimentological record that comprises the basin infill. Thus, the quantitative study of the preserved record through statistical analysis could help to unravel which source areas were actual detrital sources and, if so, the temporal variations on detrital supply.

The most prominent outcrops of Vinchina Formation occur in the Sierra de Los Colorados, where seven localities were chosen for sampling (Figs. 1 and 2). These localities were grouped into three main study sectors, namely northern, central, and southern sectors. The northern sector is represented by El Cardón, Quebrada Larga, and Los Pozuelos sections. The central one comprises Piedras Moradas, Pedregal Negro, and La Troya sections, whereas the southern sector is represented

by the El Yeso section. The mean distance between study sections is 5 km, although the El Yeso section locates 20 km southwards La Troya section.

We performed *in-situ* clasts-counting on thirty-three gravel beds belonging to channelized deposits (Schencman, 2016; Díaz, 2019). Sampling methodology (after Blatt, 1992) consisted of counting 100 to 300 clasts, from 1 to 60 cm, with random grids (Table 1). Sampling sites were chosen from fresh surfaces in order to avoid weathering effects (Bridgland, 1986). Samples and stratigraphic logs (modified from Schencman *et al.*, 2018) are presented in figure 3, providing sedimentological and stratigraphic contexts.

Clast composition was observed and categorized during field clast-counting. Primary features like rock type (sedimentary, volcanic, and/or metamorphic), color, and texture were then registered. On the basis of the observed lithologies, clasts were assigned to nine lithological classes (Table 2; Figure 4) with genetic meaning, which in turn, form conglomeratic lithic associations interpreted in terms of provenance signal: 1) reddish and dark red medium to fine-grained sandstones, named A1; 2) pink coarse-grained sandstones, named A2; 3) yellowish to greenish fine-grained sandstones, A3; 4) pink granitic rocks, named G; 5) low to high-grade metamorphic rocks, named M; 6) reddish to light purple well rounded acidic paleovolcanic rocks, Pva; 7) dark purple well-rounded intermediate to basic paleovolcanic rocks, Pvi; 8) quartz fragments and quartz aggregates, named Q; 9) grey to greenish-grey angular intermediate volcanic rocks, Nv. The latter, although volcanic in origin, makes up a separated class since this lithological class is the only one able to form monomictic conglomerates.

Descriptive statistics of compositional characteristics (mean, median, and standard deviation; Table 1) has proven that the distribution of the sampled populations is not normal. The logarithmic transformation of the original counted data (Aitchinson, 1983) did not produce fitting to a normal distribution. Thus non-parametric tests were performed, namely agglomerative hierarchical clustering and principal components analysis (PCA). The goal of applying these procedures is to compare conglomeratic deposits in order to unravel provenance indicators statistically. Cluster analysis was performed using Ward's method (Ward, 1963), which is particularly helpful in the analyzed case

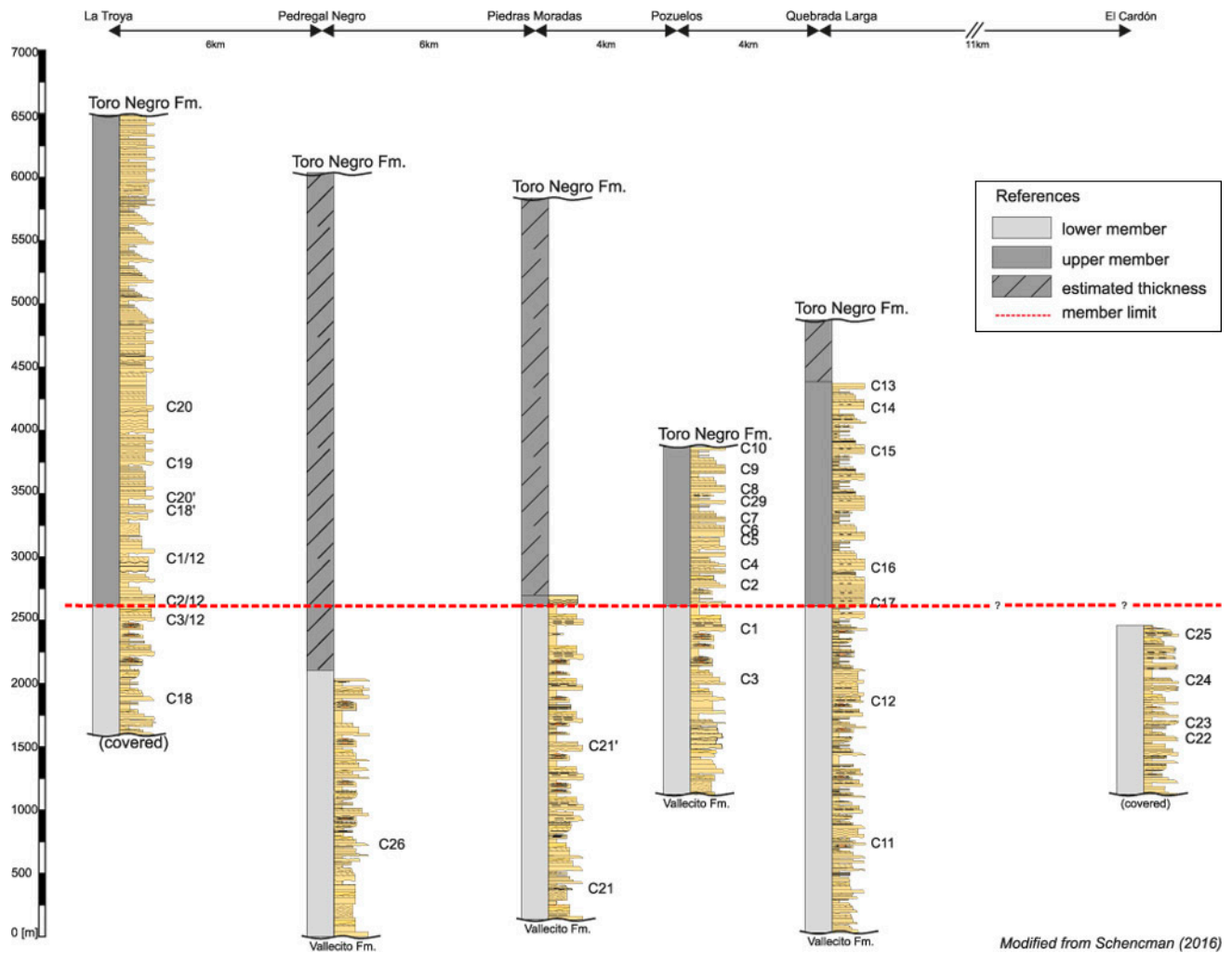


**Figure 3.** Stratigraphic location of the conglomeratic samples presented in this study (stratigraphic logs modified from Schencman, 2016). Estimated thickness was calculated from satellite imagery (Google Earth; Google LLC.)

**Figura 3.** Ubicación estratigráfica de las muestras de conglomerados presentadas en este trabajo (perfiles estratigráficos modificados de Schencman, 2016). El espesor estimado fue calculado a partir de imágenes satelitales (Google Earth; Google LLC.).

because all samples and variables are suitable for analysis, chaining is unlikely, and backward links do not occur (Mather, 1976; Young, 1986). This method's premise is that most of the information regarding the entire population is available when its n-members are ungrouped, which is indicated by a value equal to zero of the error function (*error sum of squares* - SSE) when they are ungrouped. Ward's method requires a minimum value of variance, represented by SSE, to merge clusters. The goal of this method is to use the linkage distance as a graphical expression of the similarities and dissimilarities between clusters, represented by short or long distances, respectively.

Controlling variables in cluster analysis were assessed through the conventional R-mode PCA of chord distance, with a covariance matrix with

square root transformation (Briggs and Fisher, 1986; Gibbard, 1986). PCA analysis allows quantifying the statistical significance of each variable (e.g., lithologic class) as a discriminant factor for each sample. The main goal of this method is to reduce the dimensionality of a dataset, consisting of a significant number of interrelated variables, to a smaller group of non-related variables, around which samples will cluster, and to quantify the significance of each variable in cluster formation.

Both methods were used to compare the variability between samples because the analysis quantifies the degree of similarity/dissimilarity between them. Previous works (Aitchison, 1983; Bacon-Shone, 1992; Jolliffe, 2002) argue the advantages and disadvantages of these methods when applied to

Stratigraphic location	Sample	Mean size (cm)	Maximum size (cm)	Lithological classes (%)								Cluster	
				A1	A2	A3	G	M	Pva	Pvi	Q		Nv
Northern Sector													
upper member	C10	7,0	18	16,4	4,1	2,3	6,7	10,0	14,4	32,3	0,0	13,8	2
	C9	2,5	27	15,7	5,1	2,2	8,6	20,4	13,1	16,6	0,0	18,2	2
	C13	6,0	16	17,5	0,0	0,8	4,8	17,5	9,5	11,1	0,0	38,9	3
	C8	14,0	23	13,5	0,0	2,4	2,4	2,7	12,5	27,0	0,7	38,9	2
	C29	10,0	15	0,0	0,0	0,0	0,0	0,0	0,0	0,0	0,0	100,0	1
	C7	5,0	12	15,0	3,9	2,7	10,5	4,5	19,8	29,4	0,9	13,2	2
	C6	4,0	18	10,0	3,9	3,6	18,4	15,9	23,0	24,6	0,6	0,0	2
	C5	7,5	12	11,0	2,7	3,0	18,8	26,8	14,6	22,6	0,6	0,0	3
	C14	8,0	24	12,0	0,6	1,3	4,4	15,8	16,5	15,8	0,6	32,9	2
	C15	8,0	27	8,7	0,0	2,0	11,3	44,0	26,0	6,7	1,3	0,0	3
	C4	9,0	21	13,2	6,1	2,1	16,8	34,7	14,5	8,9	3,7	0,0	3
	C2	7,0	15	28,5	4,0	4,3	21,5	17,2	12,9	9,2	0,9	1,5	3
	C16	12,0	33	5,8	4,4	0,0	5,8	42,0	28,3	12,4	1,3	0,0	3
C17	4,0	40	13,8	3,1	3,1	16,2	15,4	31,5	14,6	0,8	1,5	2	
lower member	C12	9,0	32	18,6	8,1	2,9	18,3	46,2	1,7	3,8	0,3	0,0	3
	C1	7,5	50	3,3	0,0	1,7	42,6	44,6	1,7	4,5	1,7	0,0	3
	C3	9,0	25	26,2	6,4	0,5	22,3	31,2	9,9	3,0	0,5	0,0	3
	C25	15,0	40	32,1	3,3	0,0	11,2	45,1	3,3	0,0	5,1	0,0	3
	C24	9,5	54	37,7	6,0	0,8	8,7	32,5	8,7	4,8	0,8	0,0	3
	C22	9,5	60	10,1	0,0	0,7	2,0	8,1	26,4	31,1	0,0	21,6	2
	C23	4,0	23	23,1	0,4	1,2	2,8	19,5	19,1	27,5	1,6	4,8	2
C11	2,5	17	2,2	0,0	0,9	4,4	3,5	36,7	27,9	0,4	23,9	2	
Central Sector													
upper member	C20	1,0	2,5	14,6	0,0	0,0	7,3	14,6	20,5	31,1	3,3	8,6	2
	C19	2,5	8	7,4	0,0	0,7	16,8	8,7	21,5	17,4	6,0	21,5	2
	C20'	2,0	15	0,0	0,0	0,0	0,0	0,0	0,0	0,0	0,0	100,0	1
	C18'	2,0	15	0,0	0,0	0,0	0,0	0,0	0,0	0,0	0,0	100,0	1
	C1/12	1,0	8	13,5	0,0	6,4	22,0	24,1	17,7	15,6	0,7	0,0	3
	C2/12	10,0	30	14,9	0,0	6,9	31,7	27,7	6,9	10,9	1,0	0,0	3
lower member	C3/12	2,5	22	2,5	0,0	2,0	19,9	56,2	4,5	14,9	0,0	0,0	3
	C21'	8,0	18	6,1	0,0	0,0	0,0	0,0	0,0	3,0	0,0	90,9	1
	C18	4,0	22	14,7	0,7	0,7	14,0	30,1	11,0	26,5	2,2	0,0	3
	C26	1,0	2,5	40,0	0,0	0,0	10,0	10,0	40,0	0,0	0,0	0,0	2
	C21	1,0	2,5	6,5	0,0	3,9	6,5	5,2	26,0	51,9	0,0	0,0	2
<i>Mean</i>				13,8	1,9	1,8	11,7	20,4	14,9	15,3	1,1	19,1	
<i>Median</i>				13,5	0,0	1,3	10,0	17,2	14,4	14,6	0,6	1,5	
<i>Standard deviation</i>				10,0	2,4	1,8	9,6	15,8	10,7	12,4	1,5	31,4	
<i>Variance</i>				100,9	6,0	3,1	92,1	249,0	115,1	153,8	2,1	988,8	

**Table 1.** Samples modal compositions. A1= reddish fine-grained sandstones; A2 = pink coarse-grained sandstones; A3=yellowish to greenish sandstones; G = pink granitic rocks; M = medium to high-grade metamorphic rocks; Pva = acidic paleovolcanic rocks (rhyolite); Pvi = intermediate to basic paleovolcanic rocks (basalt); Q = quartzitic metamorphic leucosome; Nv = gray to greenish gray intermediate neovolcanic rocks (andesite).

**Tabla 1.** Composiciones modales de las muestras analizadas. A1= areniscas rojizas de grano fino; A2= areniscas rosadas de grano grueso; A3= areniscas amarillentas a verdosas; G= rocas graníticas rosadas; M= rocas metamórficas de mediano a alto grado; Pva= rocas paleovolcánicas ácidas (riolita); Pvi= rocas paleovolcánicas intermedias a básicas (andesita/basalto); Q= leucosoma cuarcítico; Nv= rocas neovolcánicas de composición intermedia y color gris y gris verdoso (andesita).

Code	Description
A1	Reddish to purple, fine to medium-grained sandstones
A2	Pink coarse-grained arcose sandstones
A3	Yellowish to greenish, fine sandstones
G	Pink granitic rocks
M	Medium to high grade rocks (schist, gneiss, migmatite, amphibolite); Low-grade metamorphic rocks (slates) very subordinated
Pva	Reddish to purple, acidic volcanic rocks (rhyolite), phaneritic groundmass
Pvi	Dark purple, intermediate to basic volcanic rocks (andesite/basalt), aphanitic groundmass
Q	Quartz and quartz aggregates from metamorphic leucosome
Nv	Gray to greenish gray intermediate volcanic rocks (andesite), porphyritic texture

**Table 2.** Lithological classes: codes and descriptions.

**Tabla 2.** Clases litológicas: códigos y descripciones.

populations made up of discrete variables, which are sometimes equal to zero. That is the most common situation in modal counting, where more and better information can be obtained when PCA is applied to the original dataset (Baxter, 1993). That said, both cluster and PCA were performed on the original dataset, which comprises 33 sites with nine lithological variables.

## RESULTS

### Composition of conglomeratic beds

Conglomerates are more frequent in the northern sector of Sierra de Los Colorados; the frequency of conglomeratic levels decreases towards the central sector, whereas they are absent in the southern sector. Likewise, we have found a decrease in maximum clast-size from north to south along the depositional strike of Vinchina Basin, directly related to depositional facies distribution pattern (Díaz *et al.*, 2014; Díaz, 2019; Díaz and Marensi, 2020; Table 1). Where present, conglomerates are more frequent in the upper member than in the lower member of the unit, indicating a coarsening-upward trend.

Cluster analysis presents a cophenetic coefficient of 0.84, and it suggests the presence of three main groups. The first cluster (C1) separates from the other two at a linkage distance of 230 units, whereas the

other two (C2 and C3) separate one from the other at a linkage distance of 150 units (Figure 5). PCA of the entire population also distinguishes these three groups, indicating that 86% of the total variance is explained by PC1 and PC2, which represent Nv and M lithotypes, respectively. PC1 accumulates 69.5% of the total variation, whereas PC2 explains 17% of it (Table 3). Graphic results of PCA analysis (Aitchison y Greenacre, 2002) are presented in figure 6. First of all, Nv controls the separation of the first group in the upper-left quadrant, which coincides with cluster 1. Secondly, Pva and Pvi are the main control variables in the differentiation of the second group (the lower part of the diagram), which is partially controlled by Nv. Finally, a third group separates in the upper-right quadrant, and it is ruled mainly by M and G lithotypes, and subordinately by A1 and A2. This information is consistent with that presented by Díaz (2019) and Díaz and Marensi (2020), who, on the basis of paleovolcanic/metamorphic and neovolcanic contents, defined five petrofacies in conglomerates and sandstones of the Vinchina Formation.

Cluster 1 includes four samples (C29, C18', C20', and C21'), with compositions dominated by andesitic neovolcanic clasts (Nv lithological class). Conglomerates belonging to cluster 1 are monomictic, and their compositions are characterized by Nv contents greater than 90% (Figure 7A; Table 1).

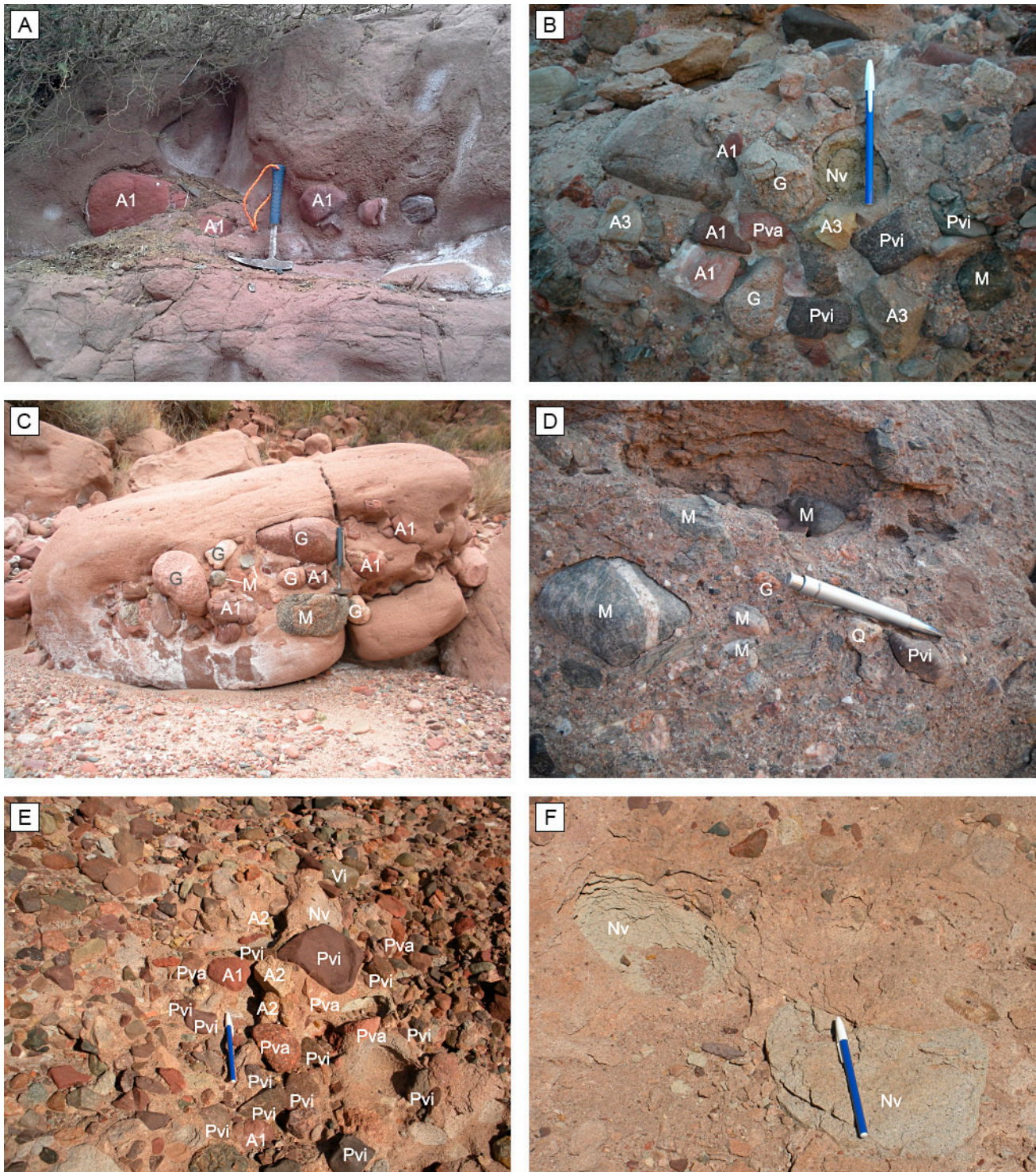


**Figure 4.** Conglomeratic lithotypes. **a)** Field photography of A1 clasts (reddish fine-grained sandstone) in blocky-sandstone layer; **b)** Clasts of A1, A3 (yellowish sandstone), Pva (rhyolite), Pvi (basalt), G (granite), M (amphibolite), and Nv (neovolcanic andesite) in a matrix-supported conglomerate; **c)** Blocks of G, M, and A1 lithotypes in a matrix-supported conglomeratic bed; **d)** Clasts of the lithotypes M (gneiss), G, Q (quartzitic leucosome), and Pvi lithotypes; **e)** Clasts of Pva, Pvi, A1, A2 (pink coarse-grained sandstone), and Nv in a clast-supported conglomerate; **f)** Nv lithotype in a pebbly sandstone.

**Figura 4.** Litotipos conglomerádicos. **a)** Fotografía de campo de clastos de A1 (arenisca rojiza de grano fino) en banco de arenisca gravosa; **b)** Clastos de A1, A3 (arenisca amarillenta), Pva (riolita), Pvi (basalto), G (granito), M (anfibilota) y Nv (andesita neovolcánica) en capa de conglomerado matriz-sostenido; **c)** Bloques de litotipos G, M y A1 en banco de conglomerado matriz-sostenido; **d)** Clastos de los litotipos M (gneiss), G, Q (leucosoma cuarácico) y Pvi; **e)** Clastos de Pva, Pvi, A1, A2 (arenisca gruesa rosada) y Nv en conglomerado clasto-soportado; **f)** Clasto de litotipo Nv en arenisca gravillosa.

	PC 1	PC 2	PC 3	PC 4	PC 5	PC 6	PC 7	PC 8	PC 9
<i>A1</i>	0,14043	0,039585	-0,77888	-0,32091	0,27041	0,23604	-0,077708	0,15209	0,33327
<i>A2</i>	0,027611	0,036411	-0,057206	-0,038476	0,063159	-0,90883	0,095281	0,20758	0,33322
<i>A3</i>	0,021227	-0,010126	0,039421	-0,093396	-0,076268	-0,10797	-0,56938	-0,73203	0,33412
<i>G</i>	0,17291	0,23092	0,20799	-0,40962	-0,70638	0,15315	-0,00077066	0,26894	0,33314
<i>M</i>	0,31359	0,60454	0,28606	0,3861	0,37648	0,16704	-0,092244	0,12685	0,33322
<i>Pva</i>	0,12679	-0,44405	-0,20318	0,69448	-0,34782	0,091653	-0,06533	0,13591	0,33324
<i>Pvi</i>	0,093867	-0,60214	0,46985	-0,28778	0,39308	0,15035	-0,0346	0,18894	0,33321
<i>Q</i>	0,012335	0,0094191	-0,0012508	0,00021394	-0,0021336	0,096075	0,80222	-0,48564	0,33333
<i>Nv</i>	-0,90873	0,13552	0,03728	0,069529	0,029485	0,12275	-0,056193	0,13955	0,33325

**Table 3.** Numerical results of PCA analysis of the entire population, showing that Nv, M, and Pvi are the main cluster-forming factors.

**Tabla 3.** Resultados numéricos del análisis de componentes principales (PCA) de toda la población, mostrando que Nv, M y Pvi son los principales factores en la conformación de los clusters.

Minor contents (less than 10%) of A1 and Pvi lithotypes are registered only in sample C21'. Figure 7B shows internal variations of this cluster, which are indicated by a linkage distance of 8-9 units, as a response to the monomictic character of these samples. PCA analysis (Figure 7C) indicates that PC1 explains 100% of the total variance, and it represents the Nv lithotype. Nevertheless, the separation of C21' sample in both clustering and PCA analysis is explained by PC2, representing the A1 lithotype in its modal composition.

Cluster 2 comprises fourteen samples (C13, C14, C8, C6, C17, C9, C19, C10, C7, C20, C23, C22, C11, and C21). This cluster involves samples of polymictic conglomerates with compositions dominated by paleovolcanic (Pva+Pvi), neovolcanic (Nv), and granitic-metamorphic clasts (Table 1). Paleovolcanic clasts' contents vary from 20 to 78%, whereas neovolcanic ones vary from 0 to 39% of total clasts. On the other hand, crystalline contributions (G+M) are present in contents from as low as 5% up to 34%. Compositional histograms (Figure 8A) of these samples show that 50% of them contain at least 15% of neovolcanic clasts. Another characteristic of this group is that 80% of the samples contain more than 10% of clasts of reddish fine-grained sandstones (A1) (Table 4). Internal variations of this cluster are

shown in figure 8B, where a linkage distance of 64 units describes the whole group. The intra-group variability was assessed utilizing PCA analysis (Figure 8C), which suggests that PC1 explains 52.8% of these variations, representing the Pvi modal component. PC2, on the other hand, explains 25.2% of the total variation, and it represents the M lithotype.

Cluster 3 involves fifteen samples (C26, C2, C3, C25, C24, C1, C12, C3/12, C5, C18, C4, C1/12, C2/12, C15, and C16). This group comprises samples with modal compositions dominated by crystalline contributions, represented by M and G lithological classes, with minor presence of paleovolcanic supply. It is essential to highlight that neovolcanic clasts (Nv lithotype) are virtually absent in these samples. Granitic-metamorphic clasts are present in contents varying between 20 and 87%, whereas paleovolcanic contributions vary from 3% to 40%. Compositional histograms obtained for these samples (Figure 9A) show the dominance of metamorphic (M) and granitic (G) contributions over paleovolcanic (Pva and Pvi) supply, which represents at least 10% of total clasts in 60% of the samples. A remarkable characteristic of cluster 3 samples is the presence of A1 clasts in more than 15% (n=7). These contents are slightly higher than those registered in cluster 3 samples (Table

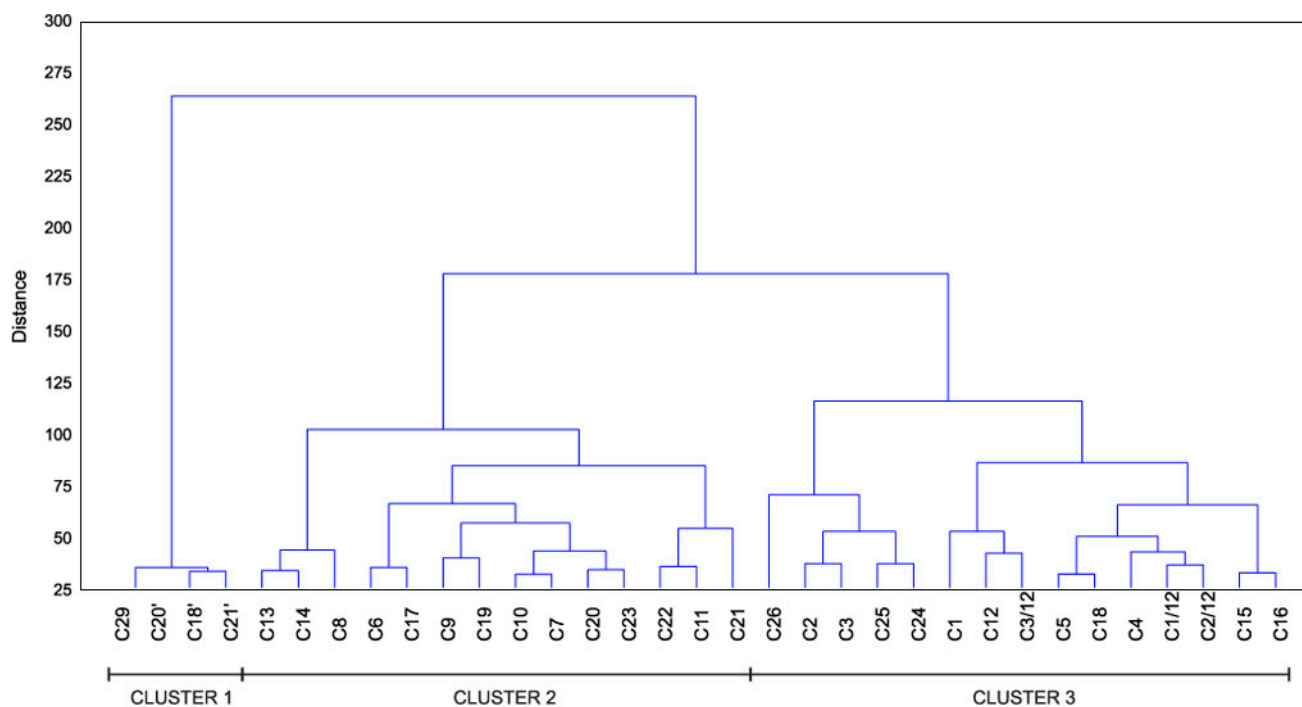


**Figure 5.** Dendrogram resulting from hierarchical cluster analysis of the entire population (after Ward, 1963). This graphic represents the three compositional groups and the samples included in them.

**Figura 5.** Dendrograma resultante del análisis de clusters de toda la población (Ward, 1963). En el gráfico se representan los tres grupos composicionales y las muestras que los conforman.

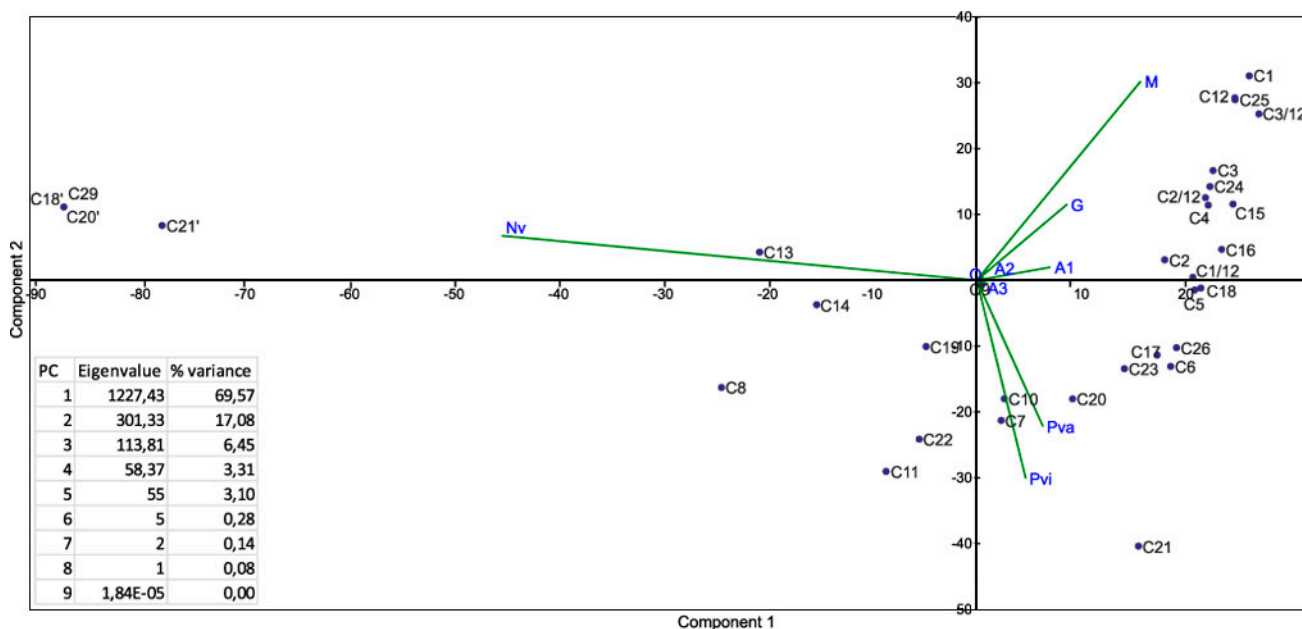


**Figure 6.** Principal components analysis (PCA) of the entire population. Samples are shown in solid blue dots; lithotypes variation vectors shown in green lines. Note the affinities between M, G, and A1 on one hand and the grouping of Pva and Pvi on the other hand. Nv separates from the main group. Mathematical results are summarized in the lower-left corner table.

**Figura 6.** Representación gráfica del análisis de componentes principales (PCA) de toda la población. Las muestras aparecen como puntos azules, mientras que los vectores de variación de los litotipos se muestran con líneas verdes. Nótese las afinidades entre M, G y A1, por un lado, y Pva y Pvi, por el otro. El litotipo Nv se separa del grupo principal. Los resultados matemáticos del análisis se encuentran resumidos en la tabla situada en la esquina inferior izquierda del gráfico.

	A1	A2	A3	G	M	Pva	Pvi	Q	Nv
cluster 1	1,52	0,00	0,00	0,00	0,00	0,00	0,76	0,00	97,73
cluster 2	12,71	1,51	1,83	7,99	11,56	20,75	25,60	1,07	16,98
cluster 3	18,04	2,78	2,22	18,32	34,18	13,45	9,58	1,34	0,10

**Table 4.** Mean composition of each cluster. Notice that cluster 1 is highly dominated by Nv contents, whereas cluster 2 and 3 are dominated by Pva+Pvi and G+M, respectively.

**Tabla 4.** Composición promedio de cada cluster. Nótese que el cluster 1 está ampliamente dominado por sus contenidos de Nv, mientras que los clusters 2 y 3 están dominados por Pva+Pvi y G+M, respectivamente.

4). The cluster diagram for this group is presented in figure 9B, with a linkage distance of 80 units. Intra-group variability is shown in the resulting PCA diagram of this cluster (Figure 9C), which indicates that PC1 accumulates 55.6% of the total variation, representing M contributions, whereas PC2 explains 22.5% of the variability, responding to variations on Pvi contents.

### Provenance interpretation

Paleovolcanic rocks clasts, Pva and Pvi lithological classes, are assigned to the erosion of volcanic rocks in Cordillera Frontal, particularly Carnerito and Ranchillos formations. In the Precordillera, Ranchillos Formation overlies Punta del Agua Formation, which is likely to have contributed with intermediate to basic paleovolcanic clasts (Fig. 2). Clasts of metamorphic-granitic origin (M, G, and Q lithotypes) are related to basement blocks (Western Sierras Pampeanas) of Sierra de Toro Negro, where Umango and Espinal formations are well developed (Fig. 2). Neovolcanic clasts (Nv) are interpreted to be intrabasinal since this is the only lithotype that is capable of constituting monomictic conglomerates, and also because Nv clasts frequently show angular/sub-angular form, forming breccia agglomerates (Diaz and Marensi, 2020). The angular shape of neovolcanic clasts is significant because it indicates short transport, which in turn, suggests that andesitic volcanic extrusions had occurred inside the basin or near its margins. Fine-grained sandstone clasts (A1 lithological class) are most likely related to the erosion of Vallecito (Eocene) and Vinchina formations. The former makes up the basement of Vinchina Basin, whereas the latter is the object of this study. Thus, it would indicate basin cannibalism during the time of

deposition. This interpretation is supported by the record of intraformational unconformities (Marensi *et al.*, 2000; 2015) and deformational episodes (Japas *et al.*, 2015, 2016). Pink, coarse-grained sandstone clasts (A2 lithological class) were assigned to Patquía/De la Cuesta formations (Neopaleozoic), whereas yellow to greenish, fine-grained sandstone clasts (A3) were assigned to Agua Colorada/Río del Peñón formations (Neopaleozoic). These units represent the infill of the Paganzo Basin, which outcrops in both the Precordillera, to the west, and Western Sierras Pampeanas, to the north. Since these lithotypes are scarce, it was not possible to confidently assign one exact origin to them.

**Clusters characterization.** Cluster 1 includes samples characterized by modal compositions largely dominated by neovolcanic clasts. This cluster is equivalent to the neovolcanic petrofacies defined by Díaz and Marensi (2020), which occurs in the upper half of the lower member of the Vinchina Formation (C21' sample) and the upper half of the upper member (C29, C18', and C20' samples). These samples result from the early reworking of contemporaneous, probably intrabasinal, andesitic rocks incorporated into fluvial streams with low transport capacity, evidenced by the low mixing degree with any other lithology. Although it is noteworthy that similar clasts are absent in both the underlying Vallecito and the overlying Toro Negro formations, the intrabasinal nature of neovolcanic clasts is still poorly understood. This interpretation is also supported by previous works (Jordan *et al.*, 1993; Kay and Mpodozis, 2002; Limarino *et al.*, 2002; Dávila *et al.*, 2004; Astini *et al.*, 2017) regarding the presence of intrabasinal andesitic/dacitic volcanic deposits in the surrounding area during the Miocene.

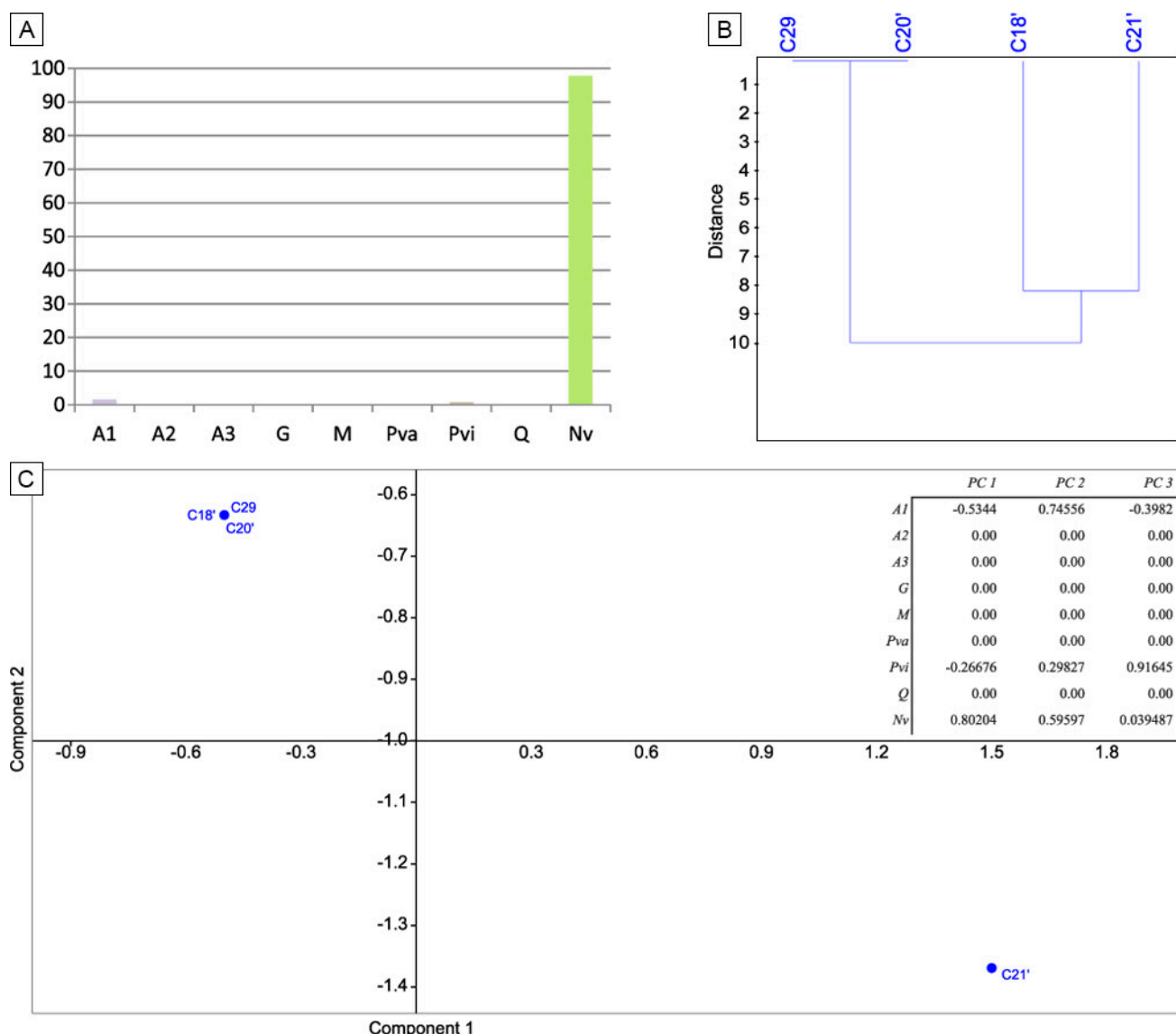


**Figure 7.** Graphic description of cluster 1. **a)** Mean contents of each lithological class, which are largely dominated by Nv clasts; **b)** Cluster analysis graphic, showing that the samples bear a high resemblance to each other, represented by a distance lower than 10 units; **c)** PCA analysis for internal variations and its numerical form.

**Figura 7.** Descripción gráfica del cluster 1. **a)** Contenido promedio de cada clase litológica, las cuales están ampliamente dominadas por clastos de Nv; **b)** Gráfico resultante del análisis de clusters, en el que se observa que las muestras presentan una alta similitud una con otra, lo cual es representado por una distancia menor de 10 unidades; **c)** Análisis de componentes principales (PCA) por variaciones internas del grupo, y su forma numérica.

Cluster 2 comprises samples with modal compositions represented by a mix of paleovolcanic, neovolcanic, and metamorphic-granitic clasts. This cluster is equivalent to the Pv and MxPv petrofacies defined by Díaz and Marenssi (2020), present in the first half of the lower member and the upper half of the Vinchina Formation. Samples of this cluster are the result of combined detrital supply from the Cordillera Frontal/Precordillera area (which contributed with paleovolcanic clasts), synchronous

-early reworked- volcanic effusions, and the crystalline basement of Western Sierras Pampeanas (Sierra de Toro Negro). It is necessary to highlight that samples of this cluster are the only ones with mixed compositions that contain neovolcanic clasts. It suggests that the andesitic neovolcanic effusions were somehow related to processes occurring in the Cordillera Frontal or Precordillera areas. In this sense, we interpret that the same streams that carried detritus from Cordillera Frontal/Precordillera are

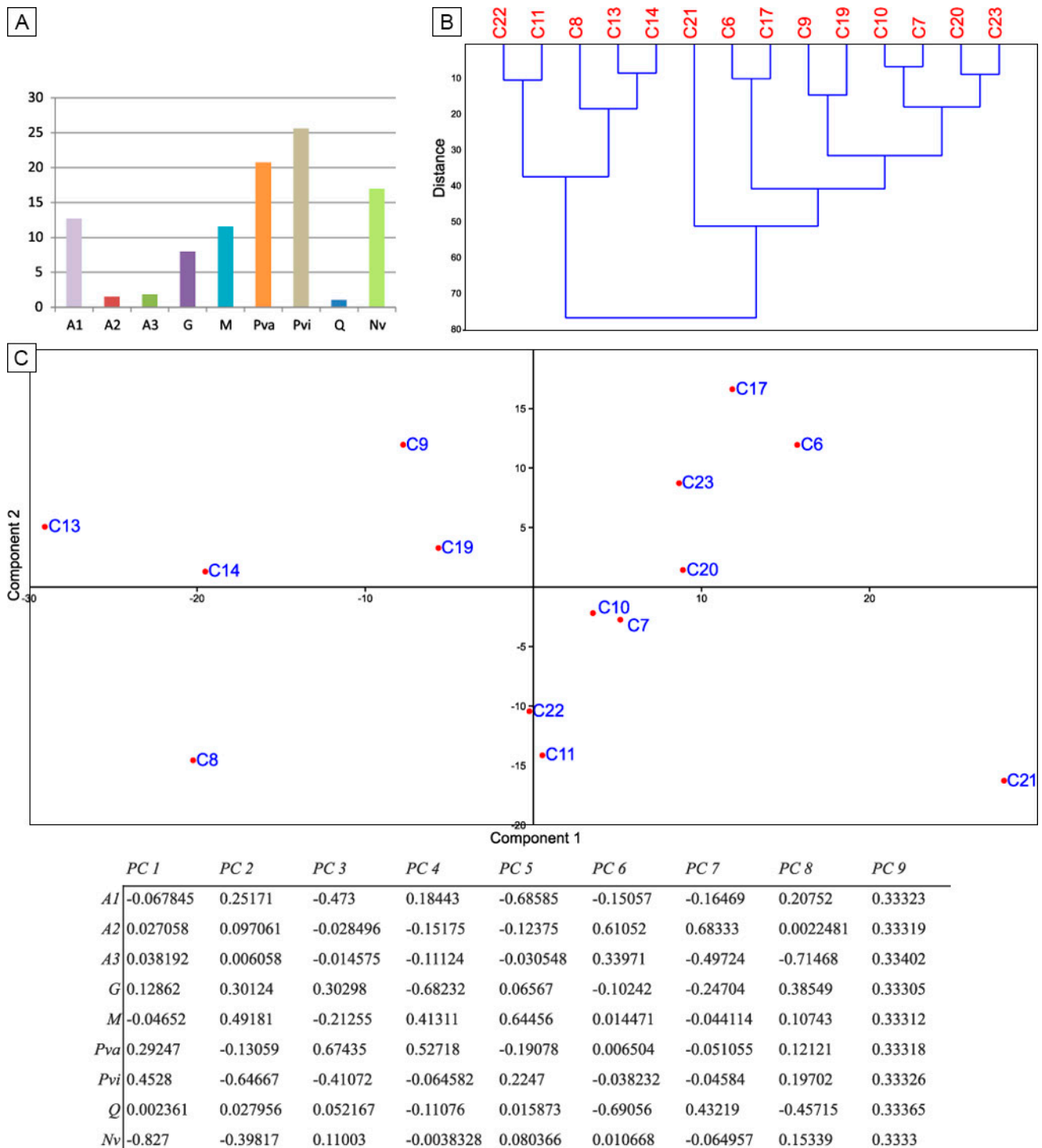


**Figure 8.** Graphic description of cluster 2. **a)** Mean contents of the lithotypes in cluster 2 samples; **b)** Dendrogram of cluster 2, which is completely formed at a distance of 75 units; **c)** Obtained PCA graph and its numerical expression for cluster 2.

**Figura 8.** Descripción gráfica del cluster 2. **a)** Contenidos medios de los litotipos en las muestras del cluster 2; **b)** Dendrograma del cluster, que se encuentra completamente diferenciado a una distancia de 75 unidades; **c)** Gráfico de PCA obtenido para el cluster 2 y su expresión numérica.

responsible for eroding the volcanic deposits that are the source of Nv lithotype. On the other hand, the presence of metamorphic clasts indicates that the

Sierra de Toro Negro was a moderately significant source area.

Samples belonging to cluster 3 represent

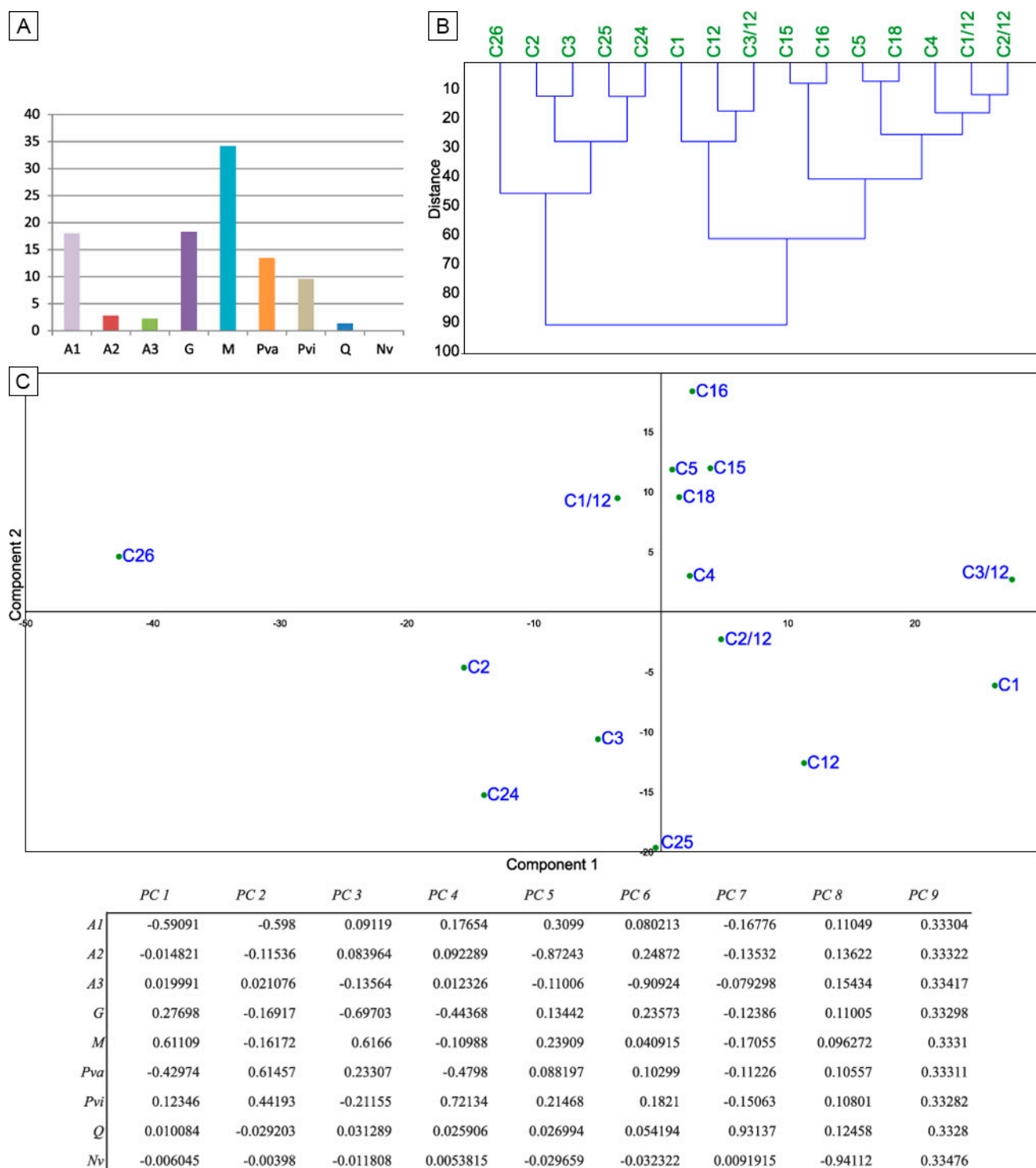


**Figure 9. a)** Histogram showing means compositions for cluster 3 (notice the absence of Nv clasts in these samples); **b)** Cluster analysis, showing that this group is formed at 90 units of distance; **c)** PCA graph and its numerical form.

**Figura 9. a)** Histograma representando las composiciones medias de las muestras del cluster 3 (nótese la ausencia del litotipo Nv en estas muestras); **b)** Análisis de clusters del grupo, mostrando que queda formado 90 unidades de distancia; **c)** Gráfico de PCA y su forma numérica).

combined contributions from the crystalline basement (M and G lithotypes) and the Cordillera Frontal/Precordillera areas (paleovolcanic Pva and

Pvi lithological classes). This group is equivalent to Bas and MxB petrofacies defined by Díaz and Marensi (2020), which are dominant in the upper

half of the lower member and the lower half of the upper member of the Vinchina Formation. A remarkable fact is that samples of cluster 3 (except for C2) do not contain neovolcanic clasts, which suggests that intrabasinal volcanic deposits were not genetically related to the crystalline source.

### **Evolution of detrital source areas**

Compositional data here presented allows the interpreting of three main stages in the evolution of the basin landscape and positive areas. The Vinchina Basin, as a broken-foreland basin, would have first developed as the flexural response to the installation of a fold and thrust belt to the west, which is represented by the Cordillera Frontal and Precordillera. Thus, these morphotectonic units were the first detrital sources of Vinchina Formation deposits, suggesting transversal drainage as the primary transport mechanism. At the same time, a basement block of Western Sierras Pampeanas (*i.e.*, Sierra de Toro Negro) acted as a secondary source area, which reflects in modal compositions of the samples of the lower half of the lower member of the unit (depositional sequence 1), which correspond to cluster 2 (samples C22, C23, C11, C21, and C26).

The base of the upper half of the lower member (depositional sequence 2) is denoted by the presence of the sample C21', which corresponds to cluster 1. Its presence suggests the synchronicity between deposition and effusive volcanism. The interval comprising the upper half of the lower member and the lower half of the upper member (depositional sequences 2 to 4) is characterized by the dominance of compositions belonging to cluster 3, which are basement-dominated. Some of the samples of the northern sector (C1, C12, C25, and C24; Table 1) show a low mixing degree with paleovolcanic rocks, whereas southwards (C3/12, C2/12, and C1/12) and along the interval (C16, C2, C4) there is a more prominent mixing. It results in the dilution of the basement signal due to contributions from the Cordillera and Precordillera. Those variations allowed interpreting the presence of a clastic wedge composed of crystalline rocks (axial drainage), resulting from the main uplifting pulse of the Sierra de Toro Negro. The occurrence of paleovolcanic clasts, even in the most basement-dominated samples, indicates that the cordilleran/precordilleran area was still providing detritus to the basin.

The base of the upper half of the upper member (sequence 5) exhibits monomictic andesitic conglomerates belonging to cluster 1. The presence of numerous monomictic conglomeratic levels in both the northern and central sectors suggests a new occurrence of synchronous effusive volcanism, with significant volcanic deposits available for transport. The rest of the upper member is characterized by samples with mixed compositions with paleovolcanic affinities belonging to cluster 2. The dominance of this cluster in this interval suggests the withdrawal of the clastic wedge due to the tectonic quiescence of Sierra de Toro Negro and a relative recovery of the paleovolcanic contributions (transverse drainage).

### **DISCUSSION**

Statistical analyses of conglomerates of the Vinchina Formation provide important information regarding the evolution of source areas and basin infill. Results here presented have significant implications for understanding variations in paleogeography and landscape evolution.

#### **Implications on provenance**

Using non-parametric statistics as an analysis tool is a new approach for understanding internal compositional trends resulting from paleogeographic variations. Cluster analysis indicates that three primary sources provided gravel clasts during the deposition of Vinchina Formation. These data are consistent with previous works, such as Tripaldi *et al.* (2001), Collo *et al.* (2017), Díaz *et al.* (2014), Díaz (2019), and Díaz and Marensi (2020). Modal compositions of conglomerates belonging to cluster 1 indicate that during the Miocene existed andesitic volcanic extrusions, which occur within the basin or its vicinity. This information is significant since there is no previous record of synchronous intrabasinal volcanism during the deposition of Vinchina Formation. Additionally, it is consistent with previous works, which registered intermediate andesitic/dacitic volcanism (Jordan *et al.*, 1993; Kay and Mpodozis, 2002; Limarino *et al.*, 2002; Dávila *et al.*, 2004; Astini *et al.*, 2017) in the surrounding areas. All these effusions attest to the eastward migration of the Andean magmatic arc as a result of the decrease in the subduction angle during the

Miocene between 27° and 33°S (Jordan *et al.*, 1993; Ramos, 1999).

Cluster 2 conglomerates exhibit substantial proportions of paleovolcanic clasts, which are interpreted as cordilleran/precordilleran in origin, consistently with the information presented by Tripaldi *et al.* (2001) and Díaz and Marensi (2020). The presence of these lithologies in lower and upper members suggests that this source area was a significant positive element and probably the most important one during the deposition of Vinchina Formation. Additionally, the occurrence of neovolcanic clasts in significant proportions suggests that the neovolcanic deposits were geographically related to the Cordillera and/or Precordillera. It makes a significant difference to cluster 3, which does not contain neovolcanic clasts.

Samples of cluster 3 show compositions dominated by basement clasts. Samples of this cluster occur almost exclusively between the upper half of the lower member and the lower half of the upper member of Vinchina Formation. This distribution is consistent with that presented by Díaz and Marensi (2020), who interpreted the progressive advance of a clastic wedge of crystalline composition from north to south, which would result from the tectonic uplift of the Sierra de Toro Negro during this time interval.

### Implications on the use of statistical methods for provenance studies

The obtained results illustrate the advantages of non-parametric statistics over the traditional methods used for provenance assessments. First, the subjective character of the traditional method *versus* the objective nature of the statistical one: the lithological grouping system on the traditional method is made on the basis of the affinities between lithological types present on the samples and the known lithological units outcropping in the source area. Thus, it is highly dependent on a thorough knowledge of potential source areas and the appropriate geological description of their units. On the other hand, hierarchical clustering groups samples with similar characteristics, in this case, lithological ones. The utilization of Ward's method (Ward, 1963) results suitable since it differentiates groups on the basis of their similarities, which is indicated by the minimum error value, which is, in turn, represented by the lowest Euclidean distance.

In the second place, PCA analysis permits to assess the relationship between lithological classes graphically. The ultimate goal in petrofacies definition is to group the lithological classes that represent a particular source area. A common obstacle when grouping under the traditional method is the presence of lithotypes present in more than one source area since there is no way to know *a priori* to which of them the operator should assign each clast. The application of multivariate analysis solves this issue since it easily permits recognizing which lithotypes are interrelated and which are not, allowing the drawn-up of more source area-representing groups.

The statistical analysis of lithological compositions has been combined with geological and stratigraphical information of the gravel deposits of Vinchina Formation (Schencman *et al.*, 2018; Díaz and Marensi, 2020). It allowed a better understanding of the behavior of the recognized lithological classes regarding their grouping or separation.

The first approach to this goal was the hierarchical clustering, which allowed separating three main compositional clusters based on their similarities and dissimilarities, expressed by distance values. The resultant clusters, when examined separately, showed that their components (samples) share similar compositions. These results were compared to those obtained by Díaz and Marensi (2020), recording an exact match between them: cluster 1 matches the neovolcanic petrofacies, cluster 2 involves the two paleovolcanic-dominated petrofacies, and cluster 3 matches the basement-dominated petrofacies (Table 5).

On the other hand, principal component analysis permitted understanding the behavior and importance of each lithological class in cluster formation. It is very significant since, although statistics is a powerful tool, a geologic control is necessary in order to avoid methodological errors. Likewise, a careful notation of the lithologies outcropping in the probable source areas is needed to carry out lithological control. Regarding this matter, PCA results indicate that Nv lithotype rules the separation of cluster 1, which is highly founded on the monomictic compositions of cluster 1 samples. Cluster 2 is governed by the contents of paleovolcanic clasts, namely Pva and Pvi, which plot together in the PCA graph. This suggests that these volcanic

Lithic components	Description	Díaz and Marensi (2020)	This work
$Nv > 90\%$	Dominated by neovolcanic clasts	Nv petrofacies	Cluster 1
$Pva + Pvi > 50\%$	Dominated by paleovolcanic clasts	$50\% < Pva + Pvi < 85\% \rightarrow$ MxPv petrofacies $Pva + Pvi > 85\% \rightarrow$ Pv petrofacies	Cluster 2
$G + M > 50\%$	Dominated by basement clasts	$50\% < G + M < 85\% \rightarrow$ MxB petrofacies $G + M > 85\% \rightarrow$ Bas petrofacies	Cluster 3

**Table 5.** Comparison between the results obtained in this work and those obtained by Díaz and Marensi (2020). The neovolcanic petrofacies proposed by the authors is represented in this work by cluster 1, whereas paleovolcanics-dominated and crystalline-dominated petrofacies are here represented by clusters 2 and 3, respectively.

**Tabla 5.** Comparación entre los resultados obtenidos en este trabajo y los obtenidos por Díaz y Marensi (2020). La petrofacies neovolcánica propuesta por los autores está representada en este trabajo por el cluster 1, mientras que la petrofacies dominada por clastos paleovolcánicos y la dominada por la presencia de clastos de origen cristalino están representadas en este trabajo por los clusters 2 y 3, respectivamente.

rocks clasts come from a geographically related area (Carnerito and Punta del Agua formations in the cordilleran/precordilleran area) and that Pvi most likely does not depict the volcanic cover of Sierra de Toro Negro, Las Planchadas Formation. Finally, cluster 3 is controlled by its crystalline-rock components, represented by M and G lithological classes, which plot together in the PCA graph. It is significant because it indicates that M and G share the source area and, more importantly, it indicates that granitic clasts are not related to the granitic plutons of the Precordillera. A more thorough analysis of these results shows that A1 lithotype is related to M and G, suggesting that red sandstones clasts correspond to the Vallecito Formation outcrops that make up part of the sedimentary cover of the crystalline basement. Since A2 and A3 are very scarce, interpretations regarding the source area of these sandstone-types would be risky.

## CONCLUSION

Although multiple source areas containing some similar lithologies posed a problem when trying to interpret provenance areas for the Vinchina Formation (Díaz and Marensi, 2020), the use of non-parametric statistical methods allowed efficiently to discriminate lithotype associations representing discrete source areas.

Three composition-based clusters were differentiated, representing the three most significant source areas of the detrital supply that reached the basin. Cluster 1 includes samples with compositions dominated by neovolcanic andesitic clasts (Nv)

and is interpreted to represent a synsedimentary and intrabasinal andesitic source, with discrete volcanic effusions. Samples of cluster 2 exhibit mixed compositions with two primary sources: a paleovolcanic one (Pva and Pvi lithological classes) and a metamorphic-granitic one (M and G). This cluster represents a cordilleran/precordilleran main supply, particularly related to the erosion of units like Punta del Agua, Ranchillos, and Carnerito formations (Figure 2). Cluster 3 involves samples with mixed modal compositions dominated by crystalline clasts (M and G) with subordinated paleovolcanic clasts (Pva and Pvi). The primary detrital source of cluster 3 is the Sierra de Toro Negro, where the metamorphic Espinal Formation outcrops (Figure 2).

These outcomes, obtained using hierarchical clustering and PCA, are entirely consistent with previous studies based on traditional techniques (Tripaldi *et al.*, 2001; Díaz and Marensi, 2020), validating the provenance interpretations.

This study proves the usefulness of using statistical methods when assessing the provenance of ancient sedimentary rocks, especially where multiple source areas share some similar lithologies, since statistical methods are more objective than the traditional one. However, a detailed and accurate dataset obtained from outcrops and regional geological knowledge is always needed, particularly in structurally complex basins such as the Vinchina Basin.

## Acknowledgments

This research work makes up a part of Dr. Díaz Ph.D. Thesis. The authors would like to thank

CONICET, Universidad de Buenos Aires, and IGeBA (UBA-CONICET) for institutional support. Likewise, we are thankful to every person who shared the field and office works with us, which allowed obtaining the information here presented. We also acknowledge careful review and helpful comments from two anonymous reviewers. This study was financed by ANPCyT PICT 1963/2014, PICT727/2012, and CONICET PIP 262/2015 research projects.

## REFERENCES

- Aitchison, J., 1983. Principal component analysis of compositional data. *Biometrika* 70: 57-65.
- Aitchison, J. and M., Greenacre, 2002. Biplots of compositional data. *Journal of the Royal Statistical Society* 51 (4): 375-392.
- Amidon, W.H., P.L., Ciccioi, S.A., Marensi, C.O., Limarino, B.G., Fisher, D.W., Burbank and A., Kylander-Clark, 2016. U-Pb ages of detrital and volcanic zircons of the Toro Negro Formation, northwestern Argentina: Age, provenance and sedimentation rates. *Journal of South American Earth Sciences* 70: 237-250.
- Astini, R.A., C.E., Colombi, J.C., Candiani, D., Kent, C., Swisher and B.D., Turrin, 2017. Aglomerados volcánicos y conglomerados volcanogénicos estratificados del Mioceno Temprano en la base de las series cenozoicas del Campo de Talampaya: Interpretación estratigráfica y significado geológico. *Revista de la Asociación Geológica Argentina* 74 (4): 423-448. Buenos Aires.
- Bacon-Shone, J., 1992. Ranking methods for compositional data. *Applied Statistics* 41: 533-537.
- Baxter, M.J., 1993. *Principal component analysis of ranked compositional data: An empirical study*. Research Report 17/93, Department of Mathematics, Statistics and Operational Research, Nottingham Trent University.
- Beer, J. A. and T. E., Jordan, 1989. The effects of Neogene thrusting on deposition in the Bermejo Basin, Argentina. *Journal of Sedimentary Petrology* 59: 330-345.
- Blatt, H., 1992. *Sedimentary Petrology*. Freeman, New York, 514 pp.
- Bridgland, D.R., 1986. *Clast Lithological Analysis*. Technical guide N°3, Quaternary Research Association, Cambridge, 207 pp.
- Briggs, D.J. and P.F., Fisher, 1986. Statistical analysis of clast lithological data. In: D.R. Bridgland (Ed.), *Clast Lithological Analysis*, Technical guide no 3. Quaternary Research Association, Cambridge, 59-72.
- Capaldi, T.N., B.K., Horton, N.R., McKenzie, D.F., Stockli and M.L., Odlum, 2017. Sediment provenance in contractional orogens: The detrital zircon record from modern rivers in the Andean fold-thrust belt and foreland basin of western Argentina. *Earth and Planetary Science Letters* 479: 83-97.
- Ciampalini, A., I., Consoloni and G., Sarti, 2011. Fault array evolution in extensional basins: insights from statistical analysis of gravel deposits in the Cecina River (Tuscany, Italy). *Sedimentology* 58: 1895-1913.
- Ciccioi, P.L., 2008. *Evolución paleoambiental, estratigrafía y petrología sedimentaria de la Formación Toro Negro, Sierras Pampeanas Noroccidentales, provincia de La Rioja*. PhD Thesis, Facultad de Ciencias Exactas y Naturales, Universidad de Buenos Aires, (inedit), 336 p., Buenos Aires.
- Ciccioi, P.L., C.O., Limarino, S.A., Marensi, A.M., Tedesco and A., Tripaldi, 2011. Tectosedimentary evolution of the La Troya and Vinchina depocenters (northern Bermejo Basin, Tertiary), La Rioja, Argentina. In: Salfity, J.A. and R.A., Marquillas, (Eds.), *Cenozoic Geology of the Central Andes of Argentina*, SCS Publisher: 91-110, Salta.
- Ciccioi, P.L., C.O., Limarino, R., Friedman and S.A., Marensi, 2014. New high precision U-Pb ages for the Vinchina Formation: Implication for the stratigraphy of the Bermejo Andean foreland basin (La Rioja province, western Argentina). *Journal of South American Earth Sciences* 56: 200-213.
- Collo, G., F.M., Dávila, W., Teixeira, J.C., Nóbile, L.G., Sant'Anna and A., Carter, 2017. Isotopic and thermochronologic evidence of extremely cold lithosphere associated with a slab flattening in the Central Andes of Argentina. *Basin Research* 29: 16-40.
- Dávila, F.M., R.A., Astini, T.E., Jordan and S.M., Kay, 2004. Early Miocene andesite conglomerates in the Sierra de Pamatina, broken foreland region of western Argentina, and documentation of magmatic broadening in the south Central Andes. *Journal of South American Earth Sciences* 17: 89-101.
- DeCelles, P.G. and K.A., Giles, 1996. Foreland basin systems. *Basin Research* 8: 105-123.
- Díaz, M., S.A., Marensi and L.J., Schencman, 2014. Análisis composicional de los conglomerados de la Formación Vinchina (Mioceno, Provincia de La Rioja). *XIV Reunión Argentina de Sedimentología*, Actas. Puerto Madryn, Chubut.
- Díaz, M., 2019. *Modas detríticas, procedencia y diagénesis de la Formación Vinchina (Mioceno), Provincia de La Rioja, Argentina*. PhD Thesis, Facultad de Ciencias Exactas y Naturales, Universidad de Buenos Aires (inedit), 479 pp. Ciudad Autónoma de Buenos Aires.
- Díaz, M. and S.A., Marensi, 2020. Using sandstone and conglomerate petrofacies to unravel multiple provenance areas in broken-foreland basins: The Vinchina Formation (Miocene, NW Argentina) as a study case. *Journal of South American Earth Sciences* 100 <https://doi.org/10.1016/j.jsames.2020.102541>
- Fauqué, L.E. and L.M., Villar, 2003. Reinterpretación estratigráfica y petrología de la Formación Chuscho, Precordillera de La Rioja. *Revista de la Asociación Geológica Argentina*, 58 (2): 218-232. Buenos Aires.
- Fauqué, L. and R., Caminos, 2006. *Hoja geológica 2969-II, Tinogasta, provincias de La Rioja, Catamarca y San Juan*. Instituto de Geología y Recursos Minerales. Servicio Geológico Minera Argentino, Boletín 276, 139 p. Buenos Aires.
- Gibbard, P.L., 1986. Comparison of the clast lithological composition of gravels in the Middle Thames using Canonical Variates Analysis and Principal Components Analysis. In: D.R. Bridgland(Ed.), *Clast Lithological Analysis* Technical guide no 3, Quaternary Research Association, Cambridge, 73-82.
- Howard, J.L., 1993. The statistics of counting clasts in rudites: a review, with examples from the upper Palaeogene of southern California, USA. *Sedimentology* 40: 157-174.
- Japas, M.S., G.H., Ré, S., Oriolo and J.F., Vilas, 2015. Palaeomagnetic data from the Precordillera fold and thrust belt constraining Neogene foreland evolution of the Pampean flat-slab segment (Central Andes, Argentina). In: Pueyo, E. L., F., Cifelli, A.J., Sussman and B., Oliva-Urcia (Eds.), *Palaeomagnetism in Fold and Thrust Belts: New Perspectives*. Geological Society of London, Special Publication no. 425. DOI: 10.1144/SP425.9.

- Japas, M.S., G.H., Ré, S., Oriolo and J.F., Vilas** 2016. Basement-involved deformation overprinting thin-skinned deformation in the Pampean flat-slab segment of the southern Central Andes, Argentina. *Geological Magazine* 153 (5-6): 1042-1065. DOI: 10.1017/S001675681600056X
- Jolliffe I.T.**, 2002. *Principal Component Analysis*, 2nd. Edition. New York. Springer. Series in Statistics. 487p.
- Jordan, T.E. and R.W., Allmendinger**, 1986. The Sierras Pampeanas of Argentina: A modern analogue of Rocky Mountain foreland deformation. *American Journal of Science* 286: 737-764.
- Jordan, T.E., R.W., Allmendinger, J.F., Damanti and R.E., Drake**, 1993. Chronology of Motion in a Complete Thrust Belt: the Precordillera, 30°-31°, Andes Mountains. *Journal of Geology* 101: 135-156.
- Jordan, T.E., F., Schlunegger and N., Cardozo**, 2001. Unsteady and spatially variable evolution of the Neogene Andean Bermejo foreland basin, Argentina. *Journal of South American Earth Sciences* 14 (7): 775-798.
- Kay, S.M. and C., Mpodozis**, 2002. Magmatism as a probe to the Neogene shallowing of the Nazca plate beneath the modern Chilean flat-slab. *Journal of South American Earth Sciences* 15: 39-57.
- Limarino, C.O. and S.R., Giordano**, 2016. Unraveling multiple provenance areas using sandstone petrofacies and geochemistry: An example in the southern flank of the Golfo San Jorge Basin (Patagonia, Argentina). *Journal of South American Earth Sciences* 66: 208-231.
- Limarino, C.O., A., Tripaldi, S.A., Marensi, L., Net, G., Re and A., Caselli**, 2001. Tectonic control on the evolution of the fluvial systems of the Vinchina Formation (Miocene), northwestern Argentina. *Journal of South American Earth Sciences* 14: 751-762.
- Limarino, C.O., L.A., Fauqué, R., Cardó, M.L., Gagliardo and L., Escoteguy**, 2002. La faja volcánica miocena de la Precordillera septentrional. *Revista de la Asociación Geológica Argentina* 57 (3): 289-304. Buenos Aires.
- Limarino, C.O., P.L., Ciccioli and S.A., Marensi**, 2010. Análisis del contacto entre las formaciones Vinchina y Toro Negro (Sierra de Los Colorados, Provincia de La Rioja, Argentina), sus implicancias tectónicas. *Latin American Journal of Sedimentology and Basin Analysis* 17 (2): 113-132.
- Marensi, S.A., L., Net, A., Caselli, A., Tripaldi and C.O., Limarino**, 2000. Hallazgo de discordancias intraformacionales en la Formación Vinchina (Neógeno), quebrada de La Troya, La Rioja, Argentina. *Revista de la Asociación Geológica Argentina* 55 (4): 414-418. Buenos Aires.
- Marensi, S.A., P.L., Ciccioli, C.O., Limarino, L.J., Schencman and M., Díaz**, 2015. Using fluvial cyclicity to decipher the interaction of basement- and fold-thrust belt tectonics in a broken foreland basin: Vinchina formation (Miocene), Northwestern Argentina. *Journal of Sedimentary Research* 85: 361-380.
- Mather, P.M.**, 1976. *Computational Methods of Multivariate Analysis in Physical Geography*. Wiley, London, 532 pp.
- Milana, J.P., F., Bercowski and T., Jordan**, 2003. Paleoambientes y magnetoestratigrafía del Neógeno de la Sierra de Mogna, y su relación con la Cuenca de Antepaís Andina. *Revista de la Asociación Geológica Argentina* 58 (3): 447-473. Buenos Aires.
- Ramos, V.A.**, 1970. Estratigrafía y estructura del Terciario en la sierra de los Colorados (Provincia de La Rioja), República Argentina. *Revista de la Asociación Geológica Argentina*, 25 (3): 359-382. Buenos Aires.
- Ramos, V.A.**, 1999. Los depósitos sinorogénicos terciarios de la región andina. In: Caminos, R., (Ed.), *Geología Argentina*. Instituto de Geología y Recursos Minerales; SEGEMAR, Anales 29 (22): 651-691, Buenos Aires.
- Schencman, L.J.**, 2016. *Arquitectura de sistemas fluviales, modelos depositacionales y estratigrafía secuencial en cuencas de antepaís: la Formación Vinchina, un caso de estudio*. PhD Thesis, Facultad de Ciencias Exactas y Naturales, Universidad de Buenos Aires (inedit), 272 pp. Buenos Aires.
- Schencman, L.J., S.A., Marensi and M., Díaz**, 2018. Evolución paleoambiental de la Formación Vinchina (Mioceno) en la Sierra de Los Colorados, La Rioja, Argentina. *Revista de la Asociación Geológica Argentina* 75 (1): 17-38. Buenos Aires.
- Stevens Goddard, A.L. and B., Carrapa**, 2017. Using basin thermal history to evaluate the role of Miocene-Pliocene flat-slab subduction in the southern Central Andes (27°S-30°S). *Basin Research* 30 (3): 564-585.
- Toselli, A.J., J., Rossi and F., Aceñolaza**, 1985. Milonitas de bajo grado de la megafractura de Sierras Pampeanas en la quebrada de La Rioja, Sierra de Velasco, Argentina. *4° Congreso Geológico Chileno* Actas, 1 (2): 159-171. Antofagasta, Chile.
- Tripaldi, A., L., Net, C., Limarino, S., Marensi, G., Re and A., Caselli**, 2001. Paleoambientes sedimentarios y procedencia de la Formación Vinchina, Mioceno, noroeste de la provincia de La Rioja. *Revista de la Asociación Geológica Argentina* 56, 443-465. Buenos Aires.
- Turner, J.C.M.**, 1964. *Descripción geológica de la Hoja 15c, Vinchina, provincia de La Rioja*: Buenos Aires, Dirección Nacional de Geología y Minería, Boletín 100, 81 p.
- Varela, A.N., L.E., Gómez-Peral, S., Richiano and D.G., Poiré**, 2013. Distinguishing similar volcanic source areas from an integrated provenance analysis: implications for foreland Andean basins. *Journal of Sedimentary Research* 83: 258-276.
- Ward, J.H.**, 1963. Hierarchical grouping to optimize an objective function. *Journal of the American Statistical Association* 58: 236-244.
- Young, R.C.**, 1986. The use of cluster analysis with stone count data. In: D.R. Bridgland(Ed.), *Clast Lithological Analysis*, Technical guide no 3, Quaternary Research Association, Cambridge, 73-82.